Article
Vol. 21, No. 1, p. 111–122, February 2017
http://dx.doi.org/10.1007/s12303-016-0041-x
pISSN 1226-4806 eISSN 1598-7477
Geosciences Journal GJ

Rock physics modelling in reservoirs within the context of time lapse seismic using well log data

Muhammad Toqeer* and Aamir Ali

Department of Earth Sciences, Quaid-I-Azam University, Islamabad 45320, Pakistan

ABSTRACT: Rock physics provides a link between seismic and reservoir properties. It helps to understand the effects of fluid substitution and reservoir parameters on seismic signatures. Rock physics models are now an integral part of feasibility study of time lapse (4D) seismic surveys and their interpretation. There exist different approaches for the construction of rock physics models within the context of 4D seismic study. The objective of this study is to investigate the predictions of existing rock physics models for time lapse seismic studies using real well data. The pore-filled fluid properties used represent the in situ conditions, while the effective elastic moduli and bulk densities are calculated based on theoretical models. Finally the reflection and amplitude predictions from each model are compared over a range of water saturation. Our results suggest that only Krief's model is able to discriminate between porous and non-porous zones effectively. Furthermore, all of the investigated models show increase in velocity with replacement of oil with heavier fluid i.e., water except Wyllie's model. There is a significant change in seismic amplitude when compared with in situ conditions for this particular lithology.

Key words: rock physics modelling, 4D seismic, fluid substitution, reflectivity, amplitude

Manuscript received June 22, 2015; Manuscript accepted May 7, 2016

1. INTRODUCTION

Hydrocarbon reservoir management is a key task during the development phase. Time lapse (4D) seismic surveys are repeated three dimensional (3D) seismic surveys used for monitoring and quantifying changes in seismic properties of saturated rocks (Biondi et al., 1998; Blonk et al., 1998; Sengupta et al., 2003; Johnston, 2013). Monitoring and quantification of changes in reservoir properties require construction of proper rock physics models (Watts et al., 1996; Nguyen and Nam, 2011). Construction of rock physics models accomplishes the initial task of feasibility study for analysis of 4D seismic by manifesting the changes in seismic, production or injection related properties at specific reservoir conditions (Benson and Cole, 2008; Kazemeini et al., 2010). Through the forward modelling based on rock physics models, the simulated seismic response helps to understand the effect of fluid substitution, change in stress regime and elastic properties of the reservoir at different injection and production stages (Mavko et al., 1995; Mezghani et al., 2004; Li, 2009).

Moreover, interpretation of 4D seismic is facilitated based on rock physics models to understand the change in fluid saturation, pressure, temperature and other reservoir parameters that are responsible for change in seismic signatures at a particular stage (Tsuneyama and Mavko, 2007).

Numerous empirical relationships and theories are proposed to link the reservoir parameters and seismic signatures of reservoir rocks. Due to different depositional and post depositional processes that further alter the porosity, grain morphology, fracturing and packing, different rock physics models are proposed for carbonates and clastic reservoirs (Misaghi et al., 2010; de Paula et al., 2010).

The objective of this study is to investigate and compare the predictions of four different rock physics models using real well data within the context of 4D seismic study. These models include Gassmann (Gassmann, 1951), Krief (Krief et al., 1990), Duffy-Mindlin (Duffy and Mindlin, 1957) and Wyllie (Wyllie et al., 1956; Wyllie et al., 1958). The data recorded in the Chak-7A well located in the Sanghar area of the Lower Indus Basin,

*Corresponding author:
Muhammad Toqeer
Department of Earth Sciences, Quaid-I-Azam University, Islamabad 45320, Pakistan
Tel: +92-51-90642164, Fax: +92-51-90644087,
E-mail: mtoqeerpk@gmail.com

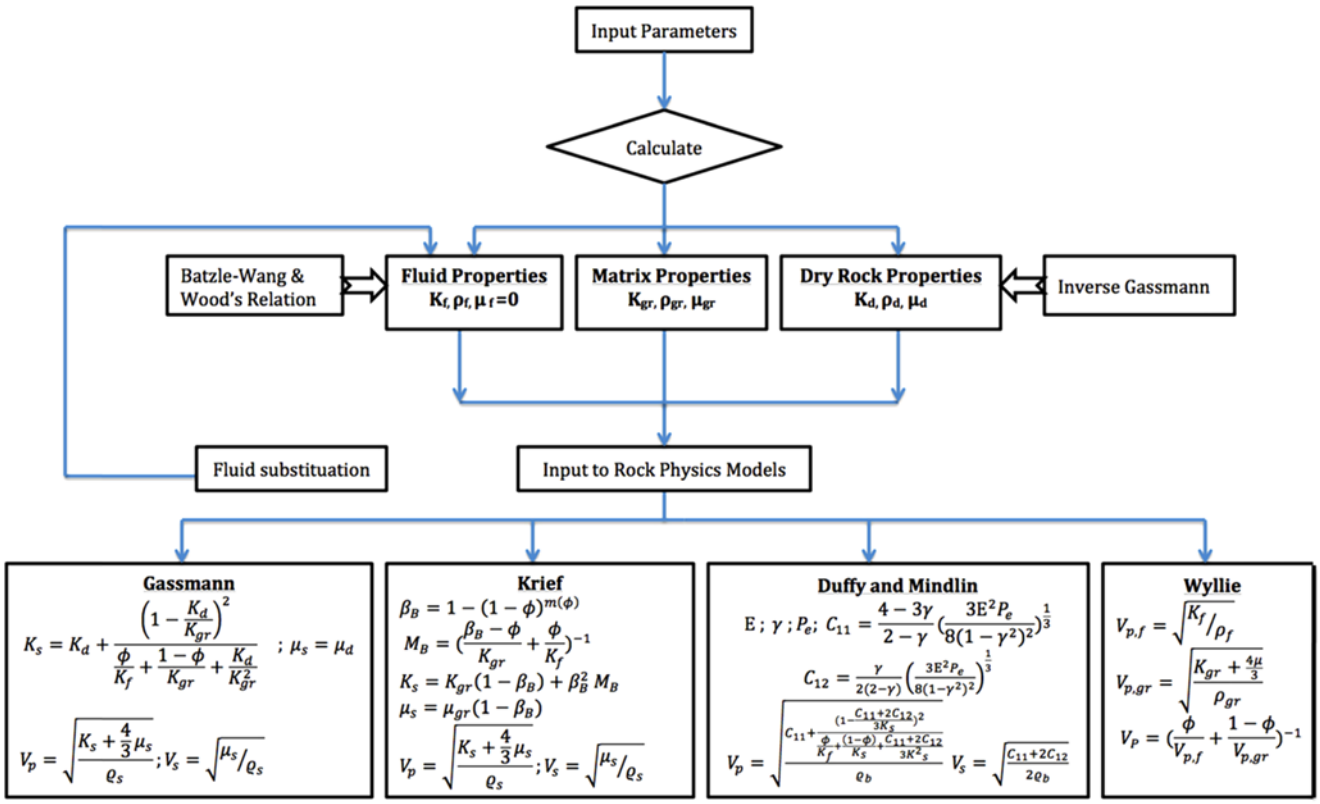

Fig. 1. Simple flowchart of different rock physics models. The end product is V_P velocity at different water saturations.

Pakistan is used to investigate and compare the predictions of the four different rock physics models being examined. The methodology used to accomplish the objectives is presented in the workflow shown in Figure 1.

The study area (Fig. 2) is dominated by extensional horst and graben structural features favourable for hydrocarbon accumulations. The tectonic framework and geology of the area are detailed in Akhter et al. (2014). Early/Middle Cretaceous sands of the Goru Formation are well developed and act as a major hydrocarbon reservoir (Kadri, 1995). The stratigraphy of the study area is shown in Figure 3. Figure 4 shows: 1) P-wave velocity, 2) empirically estimated S-wave velocity (Mavko et al., 2009), 3) density and porosity logs from the Chak-7A well, used as input data for fluid substitution. The following we present a brief introduction of four different rock physics models used in this study.

2. CALCULATION OF CORE PARAMETERS FOR 4D ROCK PHYSICS MODELING

The basic constituents required for the construction of rock physics models are elastic moduli of matrix, dry rock and fluid along with their bulk densities (Avseth et al., 2005). The elastic moduli of matrix and dry rocks may be measured in lab or estimated from the wireline well logs.

A grain is an amalgamate of different minerals. Each mineralogical component has specific properties, modulus and density, which affect the seismic signatures. With known properties and fractional volumes of each mineral the density and modulus of the grain phase is approximated. The density of aggregate ρ_{gr} is simply the weighted sum of the densities $\rho_{gr,i}$ and respective fractional volume V_i of individual components.

$$\rho_{gr} = \sum_{i=1}^{N} V_i \rho_{gr,i}. \quad (1)$$

Similarly to calculate the effective grain moduli (bulk and shear) for matrix, different bounds and consequent mixing laws are proposed by Hill (1952) and Hashin and Shtrikman (1963).

Voigt-Reuss-Hill (M_{VRH}) averaging is a simple method to calculate the effective bulk moduli of matrix. It is basically the average of Voigt upper (M_V) and Reuss lower (M_R) bounds given as (Hill, 1952; Mavko et al., 2009):

$$M_{VRH} = \frac{M_V + M_R}{2}, \quad (2)$$

where

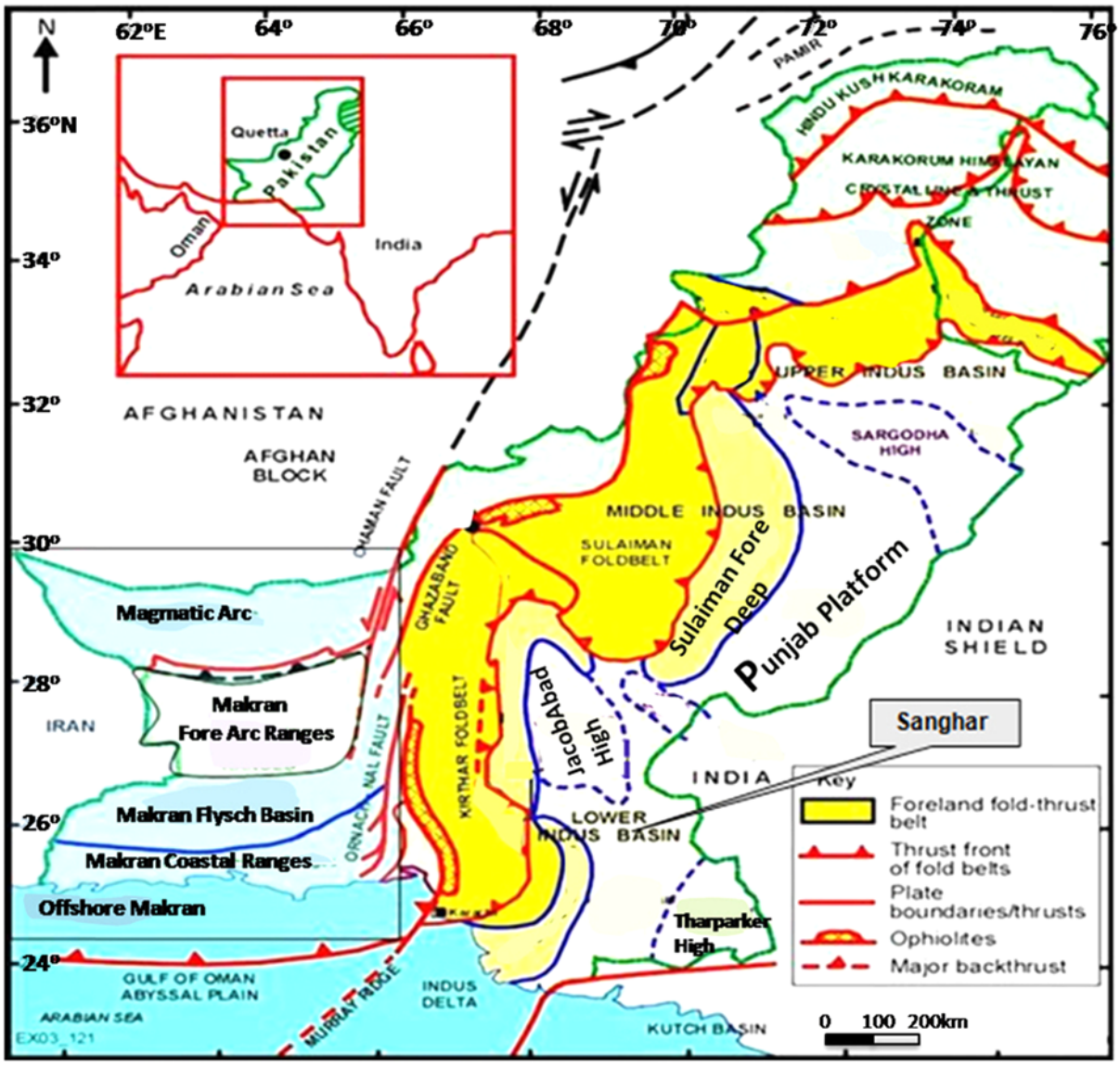

Fig. 2. Map showing the annotated location and tectonic framework of the study area (Banks and Warburton, 1986).

$$M_V = \sum_{i=1}^{N} V_i M_i, \tag{3}$$

and

$$\frac{1}{M_R} = \sum_{i=1}^{N} \frac{V_i}{M_i}. \tag{4}$$

These bounds and averaging predict the behaviour grossly. More accurate values may be calculated by taking into account the geometrical details related with sorting and packing (Mavko et al., 2009).

Dry rocks are bare of any fluid, so their properties are function of pores and grains. Density for dry rock ρ_d is computed simply by:

$$\rho_d = \varphi \rho_{gr}. \tag{5}$$

Due to the influence of lithology, grain shape, structure, texture and pore spaces the effective moduli determination for dry rocks is quite difficult. Laboratory measurements of core samples give the best estimation of effective moduli for dry rock, however in the absence of the aforementioned measurements one must rely on the empirical relations and theoretical models developed to address the problem (Mavko et al., 2009). Empirical relations used for this purpose are mostly based on the relationship between moduli and grain porosity (Biot, 1956; Geertsma and Smit, 1961; Murphy, 1982; Jones and Nur, 1983; Castagna et al., 1985; Han et al., 1986).

In this study the bulk modulus of dry rock K_d is calculated from well logs at each depth sample by Gassmann's (Zhu and

http://dx.doi.org/10.1007/s12303-016-0041-x

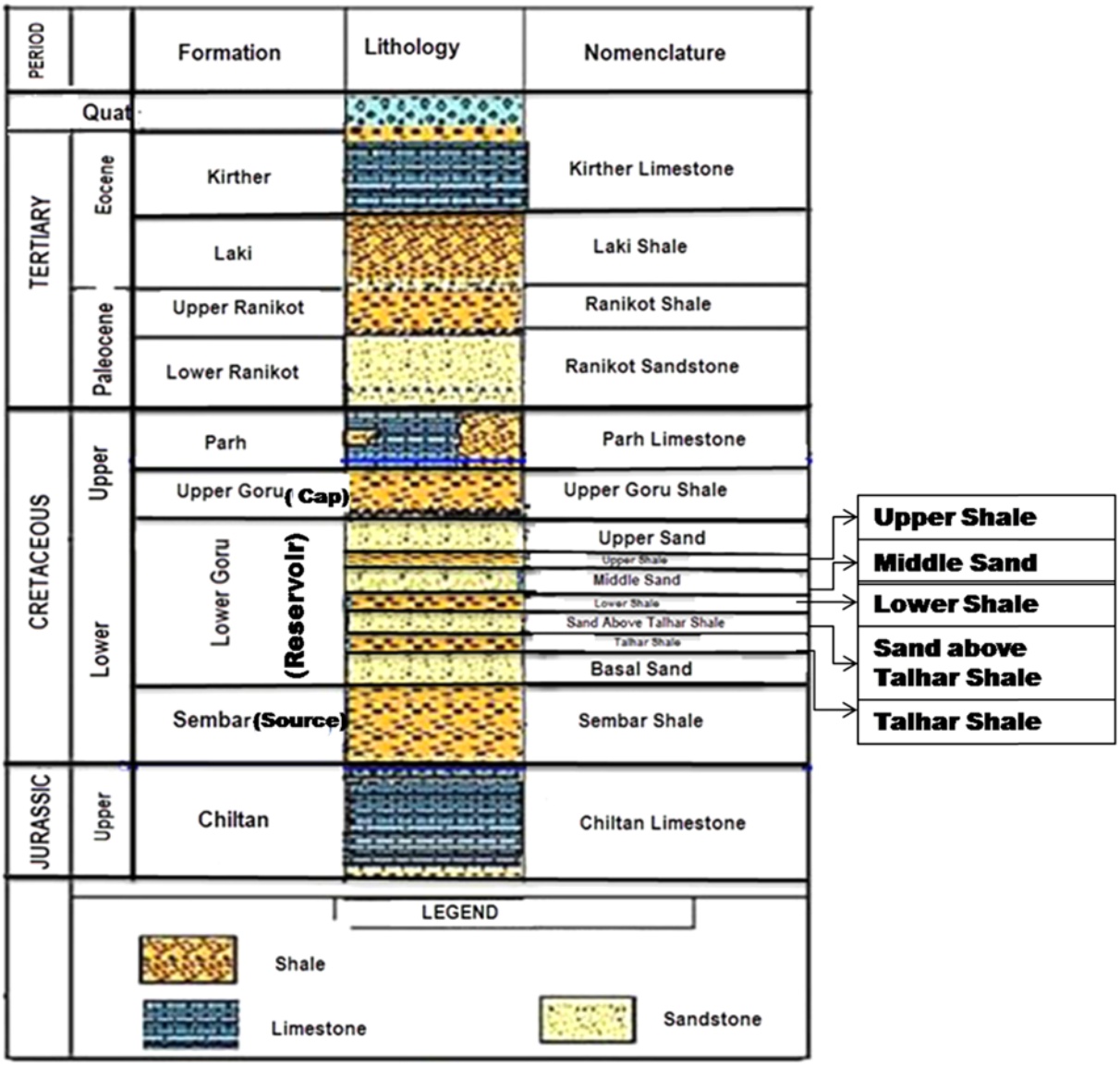

Fig. 3. Stratigraphic chart of the study area showing the petroleum play (Zaigham and Mallick, 2000).

McMechan, 1990; Wang, 2001) backward substitution method. Gassmann's relation, Equation (8), relates bulk modulus of saturated rock, porosity, and bulk modulus of rock frame, mineral and pore fluids.

The pore-fluid properties, brine water, oil and gas are determined at in situ conditions namely temperature, pressure, salinity and viscosity amidst other using the relation given by Batzle and Wang (1992). The effective bulk moduli K_f and density ρ_f of the reservoir fluids are given by (Wood, 1955; Kumar, 2006):

$$K_f = \left(\sum_{i=1}^{N} S_i K_{f,i}^{-1}\right), \tag{6}$$

and

$$\rho_f = \left(\sum_{i=1}^{N} \rho_i S_i\right). \tag{7}$$

Here N is number of fluid phase component that may be water, oil or gas. S_i and K_{fl} are saturation and bulk modulus of respective fluid phase.

The applicability of these core parameters for each rock physics model is given in the schematic workflow presented in Figure 1.

2.1. Gassmann's Model

Gassmann's equation (Gassmann, 1951) is the most widely used relation to construct the saturated rock physics model (Lumley, 2001; Artolaand Alvarado, 2006; Landrø, 2006; Mavko

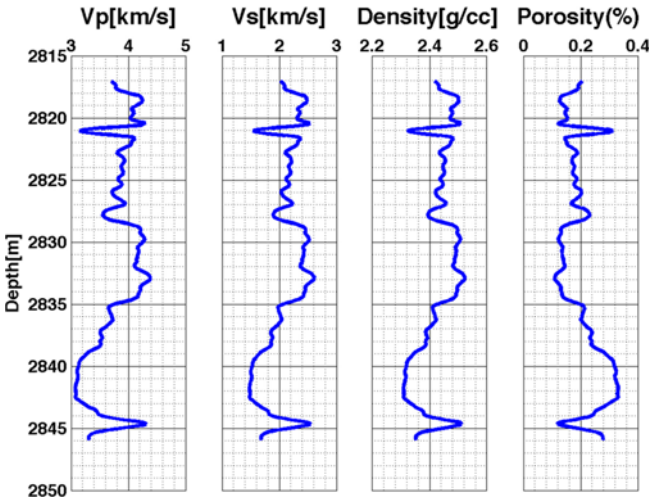

Fig. 4. Chak 7A-1 well log curves through the studied reservoir interval. The S-wave velocity is estimated by using the empirical relation $V_s = 0.804V_p - 0.856$ (Mavko et al., 2009).

et al., 2009; Nguyen and Nam, 2011). According to Gassmann's equation, saturated rock bulk modulus is a function of porosity, bulk modulus of rock frame, mineral and pore fluids (Adam et al., 2006; Simm, 2007; Mavko et al., 2009). Mathematically it can be written as (Mavko et al., 2009):

$$K_s = K_d + \frac{\left(1-\frac{K_d}{K_{gr}}\right)^2}{\frac{\varphi}{K_f}+\frac{1-\varphi}{K_{gr}}+\frac{K_d}{K_{gr}^2}}, \tag{8}$$

where K_s, K_d, K_{gr}, K_f are bulk moduli of saturated rock, dry rock, grains and fluid, respectively, and φ is the porosity. Since the presence of fluid has negligible effects on the shear modulus of the saturated rock, it is assumed:

$$\mu_s = \mu_d, \tag{9}$$

where μ_s and μ_d are shear moduli of saturated and dry rocks, respectively. Certain underlying assumptions (Wang, 2001; Han and Batzle, 2004; Misaghi et al., 2010) of Gassmann's theory are: 1) Both frame and rock matrix of a rock should be homogeneous at macroscopic scale; 2) interconnectivity of all pores; 3) pore filling fluid must be frictionless; 4) the rock-fluid system must be undrained; and 5) softening or hardening of cavities should not be at the expense of fluid and matrix interaction. From Equations (1) and (2), saturated bulk and shear moduli can be calculated which are further used to compute V_p and V_s given as (Kumar, 2006):

$$V_P = \sqrt{\frac{K_S+\frac{4}{3}\mu_S}{\rho_S}}, \tag{10}$$

and

$$V_s = \sqrt{\frac{\mu_s}{\rho_s}}, \tag{11}$$

where ρ_s is density of saturated rock expressed as:

$$\rho_s = \varphi\rho_f + (1-\varphi)\rho_{gr}. \tag{12}$$

2.2. Krief's Model

Biot's coefficient M_B and Biot's compressibility β_B constants (Biot, 1941) are used to drive the moduli of grain for the construction of the Krief's model (Krief et al., 1990). This model employs empirical relations between Biot's coefficients and porosity φ given by (Goldberg and Gurevich, 1998):

$$\beta_B = 1-(1-\varphi)^{\left(\frac{3}{1-\varphi}\right)}, \tag{13}$$

and

$$M_B = \left(\frac{\beta_B-\varphi}{K_{gr}}+\frac{\varphi}{K_f}\right)^{-1}. \tag{14}$$

The bulk and shear saturated moduli then can be calculated using the relations given by (Nguyen and Nam, 2011):

$$K_S = K_{gr}(1-\beta_B)+\beta_B^2 M_B, \tag{15}$$

$$\mu_S = \mu_{gr}(1-\beta_B). \tag{16}$$

Krief's model facilitates the rock physics model construction and does not require computation of the dry rock modulus. Using Equations (15) and (16) V_P and V_S can be calculated using Equations (10) and (11).

2.3. Duffy and Mindlin's Model

Duffy and Mindlin's (Duffy and Mindlin, 1957; Varela et al., 2006) model is based on the effective pressure, porosity, lithology and mechanical compaction. Saturated velocities are calculated as a function of Young's modulus E and Poisson's ratio ν which are given by (Varela et al., 2006):

$$E = \frac{9K_d\mu_d}{3K_d+\mu_d}, \tag{17}$$

$$\nu = \frac{3K_d-2\mu_d}{2(3K_d+\mu_d)}. \tag{18}$$

The velocities V_P and V_S are given in the following form

$$V_P^2 = \frac{C_{11}+\frac{\left(1-\frac{C_{11}+2C_{12}}{3K_s}\right)^2}{\frac{\varphi}{K_f}+\frac{1-\varphi}{K_s}+\frac{C_{11}+2C_{12}}{3K_s^2}}}{\rho_b}, \tag{19}$$

http://dx.doi.org/10.1007/s12303-016-0041-x

$$V_S^2 = \frac{C_{11} + C_{12}}{2\rho_b}. \quad (20)$$

C_{11} and C_{12}, represent the combination of mechanical parameters in terms of Young's modulus and Poisson's ratios, introduced in above equations are calculated as:

$$C_{11} = \frac{4-3\nu}{2-\nu}\left(\frac{3E^2P_e}{8(1-\nu^2)}\right)^{\frac{1}{3}}; C_{12} = \frac{\nu}{2(2-\nu)}\left(\frac{3E^2P_e}{8(1-\nu^2)^2}\right)^{\frac{1}{3}}, \quad (21)$$

where P_e denotes the effective pressure.

2.4. Wyllie's Time Average Equation

For a mono-mineralic rock Wyllie's equation (Wyllie et al., 1956; Wyllie et al., 1958) assumes that the total transit time is simply the sum of transit times in the corresponding pore-phase and matrix-phase. Mathematically it is written as (Guéguen. 1994):

$$\frac{1}{V_P} = \frac{\varphi}{V_{P,f}} + \frac{1-\varphi}{V_{P,gr}}, \quad (22)$$

where

$$V_{P,f} = \sqrt{\frac{K_f}{\rho_f}}, \quad (23)$$

and

$$V_{P,gr} = \sqrt{\frac{K_{gr} + \frac{4}{3}\mu_{gr}}{\rho_f}}. \quad (24)$$

Here $V_{P,f}$ and $V_{P,gr}$ stands for P-wave velocity through the fluid and matrix, respectively. Wyllie's time average method is the only one of the rock physics models that ignored V_S.

Despite its simplicity and convenience for estimation of the seismic velocity over the reservoir zone, this equation is constrained to the case where there exists, gas filled pores, incomplete lithification, presence of fractures and spherical or near spherical pore-space geometry (Guéguen, 1994; Saleh and Castagna, 2004).

3. RESULTS AND DISCUSSIONS

In this section we present the results from investigation and prediction of four widely used rock physics 4D seismic models.

Table 1. Moduli and densities of the material

Material	Bulk Modulus (GPa)	Shear Modulus (GPa)	Density (g/cc)
Clay	20.9	7	2.58
Quartz	36.6	45	2.6

Table 2. Input parameters, fluid and petrophysical properties

	Properties	Values
Fluid	Oil gravity	51 API
	Gas oil ratio	160.0
	Gas gravity	0.79 API
	Temperature	135 C
	Pressure	28.6 MPa
	Salinity	20000 ppm
Reservoir	Well average porosity	20%
	Initial Water Saturation	40%
	Volume of Shale	14%
	Volume of Quartz	86%

Matrix properties are calculated using Voiget-Reuss approximation. The constituent grain properties are listed in Table 1. Table 2 shows the in situ condition reservoir fluid properties used within the Batzle and Wang's (1992) relation to calculate the effective fluid properties. The bulk modulus for dry rock K_d is calculated from Gassmann's relation whereas the initial saturated modulus K_s and porosity φ is estimated from the well log data. The response of each model is calculated to different fluid saturations to those found in situ. The process of core parameters calculation and subsequent rock physics model preparation is outlined in the flow chart of Figure 1. Figure 5 shows the forward modelling obtained from the well data at in situ conditions. More specifically, sonic, density log and a Ricker wavelet of 30 Hz are used for 1D forward modelling purpose. The same Ricker wavelet and procedure is used to generate synthetic seismic traces from the output of rock physics models.

The results of these rock physics models are presented and compared in different perspectives. Firstly the results of each model are presented and compared for a range of water saturations in terms of velocity and secondly for a range of specific water saturation scenarios. The modelled results are cross examined and the synthetic seismic traces of these rock physics models

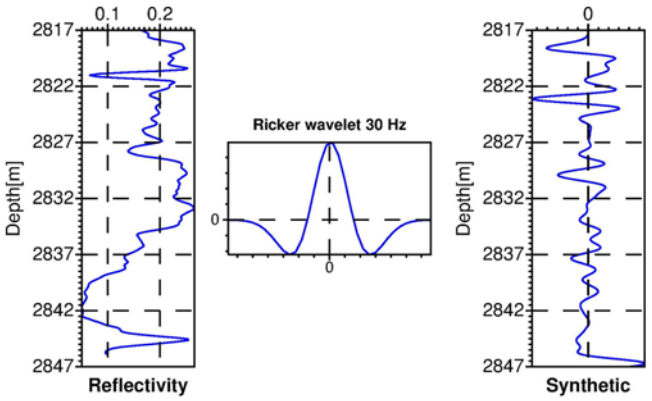

Fig. 5. 1D forward modelling of well driven reflectivity at initial water saturation of 40%.

are computed and discussed at specific water saturation scenarios.

Once the dry modulus is calculated at the initial fluid saturation, 40% water saturation and 60% oil saturation, it held constant afterwards for fluid substitution. For fluid substitution purpose oil is replaced by brine water. For example at 10% water saturation, 90% oil is present, then oil is replaced sequentially by water such that 20% water and 80% oil, 30% water and 70% oil untill oil is replaced fully by water, which is the situation for 100% water saturation. Figure 6 shows the velocities after fluid substitution from 10% to 100% water saturation levels at an interval of 10%; obtained from different rock physics models (Gassmann, Krief, Duffy and Mindlin, and Wyllie). The original well velocity is also plotted as a reference. Each figure is zoomed and plotted as indicated by the red rectangles in the corresponding subplots for clear visualization.

For Gassmann's model (Fig. 6a), the effect of different water saturations is manifested by the velocities in the graph. Although the velocity increases with increasing water saturation but at few water saturations the velocity also decreases. The maximum velocity corresponds to 100% water saturation. The velocity calculated from the model at the 40% water saturation is largely greater than the velocity recorded in the well at the same saturation. The lowest velocity is at 70% saturation while the velocity increases at 60% and 80% respectively. Furthermore the velocities still increase for the lower water saturations in an inverse manner such that for 10% water saturation the velocity is nearest to the velocity at the 100% water saturation. The velocities approach their lower limit from 20 to 60% water saturations.

For Krief's model (Fig. 6b), two observations are made at two different depth intervals. The velocities for all water saturations are greater than well velocity except in the most porous zone

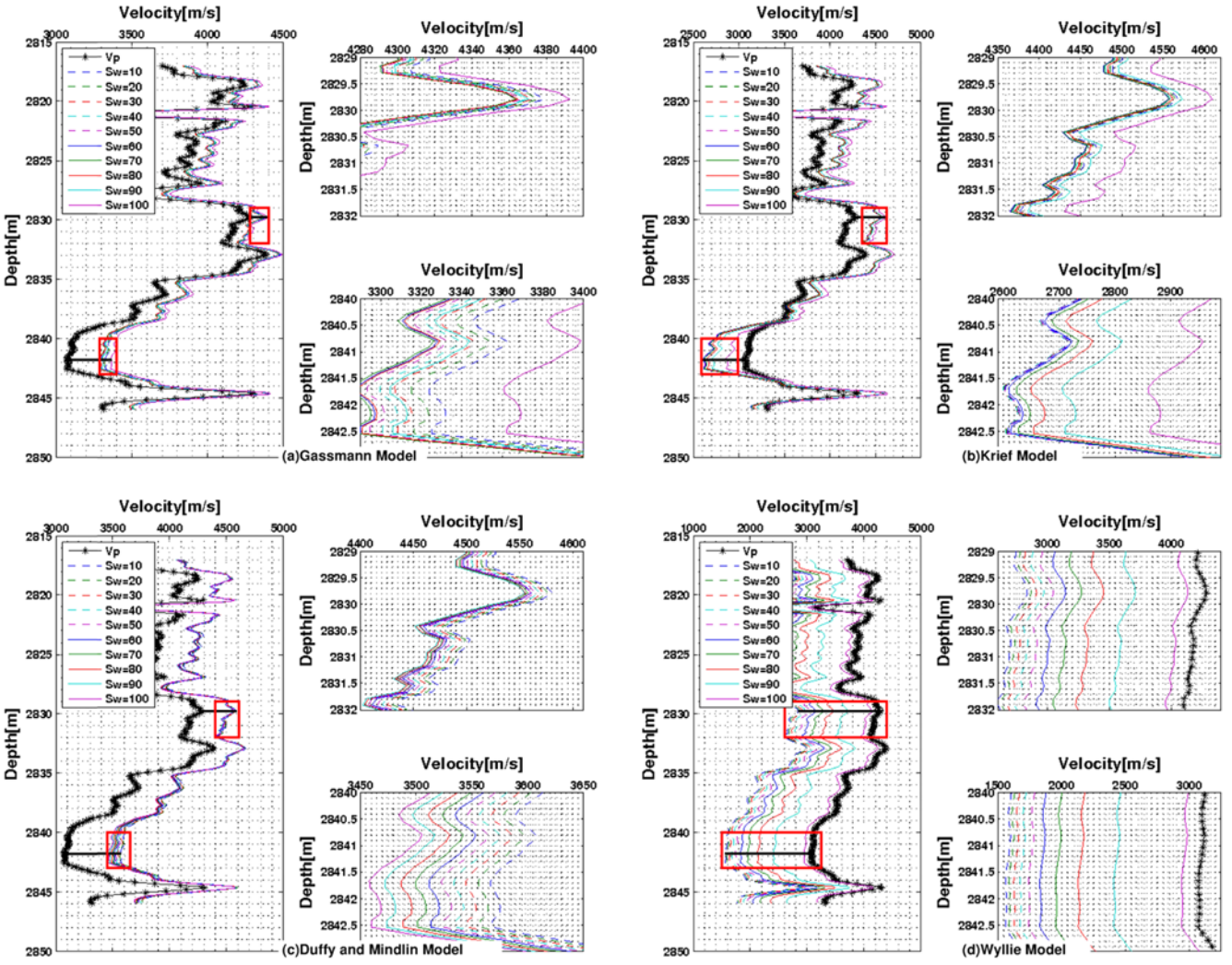

Fig. 6. Rock Physics Templates. The response of each rock physics model is calculated for water saturation from 10% to 100%. The red boxes are the zoomed locations that are shown in the right side of each model. The black line in each red box corresponds to the depth point for which the water saturation is plotted as a function of velocity. The well velocity is also plotted for each particular rock physics model as a reference to see the velocity variation as a function of saturation.

http://dx.doi.org/10.1007/s12303-016-0041-x

from 2838–2844 m depth interval. Though at 100% water saturation highest velocity is observed but as expected the velocities should increase with increasing water saturation is not attained. The lowest velocity after fluid substitution is at 60% water saturation. For the most porous zone the velocities increase in a uniform manner for the water saturation from 60 to 100% but nonetheless remain below the velocity calculated from the well logs. This phenomenon may be attributed to the Biot's compressibility factor, which is heavily porosity dependent as given in Equation (13).

For Duffy-Mindlin's model (Fig. 6c), although the maximum velocity is at 100% water saturation but for the rest of the different water saturations scenario there is no clear trend. In the most porous zone the velocities are decreasing for increasing water saturations. The highest velocity corresponds to the 10% water saturation while for the increasing water saturations the corresponding velocities decrease in a regular manner. The velocity variation lies in a close range between 3450 to 3625 m/s. For Wyllie's model (Fig. 6d) the velocities at all water saturations are lesser than the velocity at in situ condition, however only this model results in the velocities increasing systematically for the increasing water saturation. Even for the 100% water saturation the velocity is lesser than the well velocity. For the lower water saturations the difference among the corresponding velocities is small and this difference in velocity increases with the increase of water saturation. In the most porous zone at all water saturations there is a considerable decrease in velocities. This phenomenon may be attributed to the simplicity of the model, as it simply takes into account the transit times in the solid and fluid.

Figure 7 shows the V_P as a function of water saturation for two different depth points. Note the velocity range, the lower and upper limit of velocity, is higher in less porous zone (Fig. 7a) as compared to the more porous zone (Fig. 7b) which is expected. Wyllie's model shows the similar trend in both scenarios i.e., the velocity increases with increasing water saturation (Figs. 7a and b). For both scenarios, Gassmann's model shows slight increase in velocity with increasing water saturation but the velocity values for more porous zone are considerably lower than in low porous zone (Figs. 7a and b).

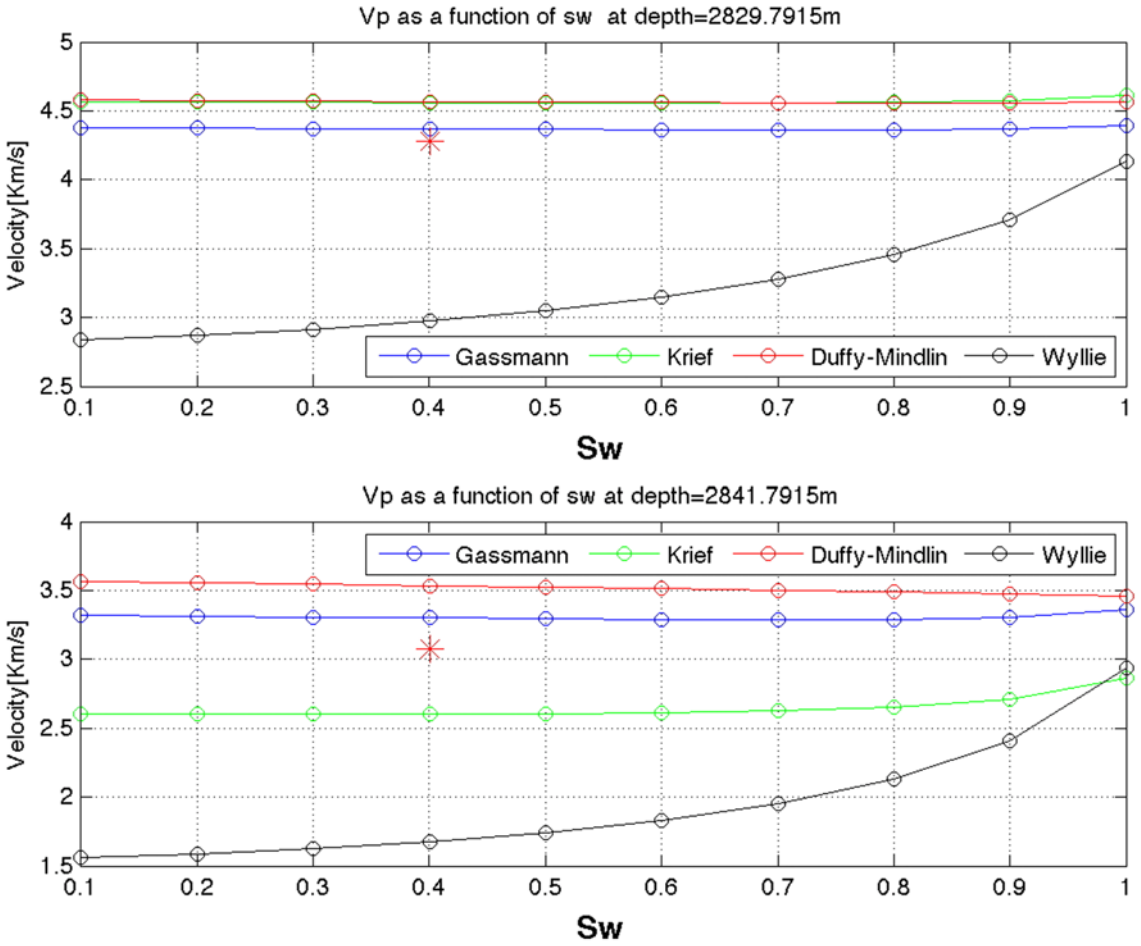

Fig. 7. Velocity as a function of water saturation (sw) at particular depth intervals as indicated by black lines in Figure 6. The red asterisk indicates the well velocity at 40% water saturation.

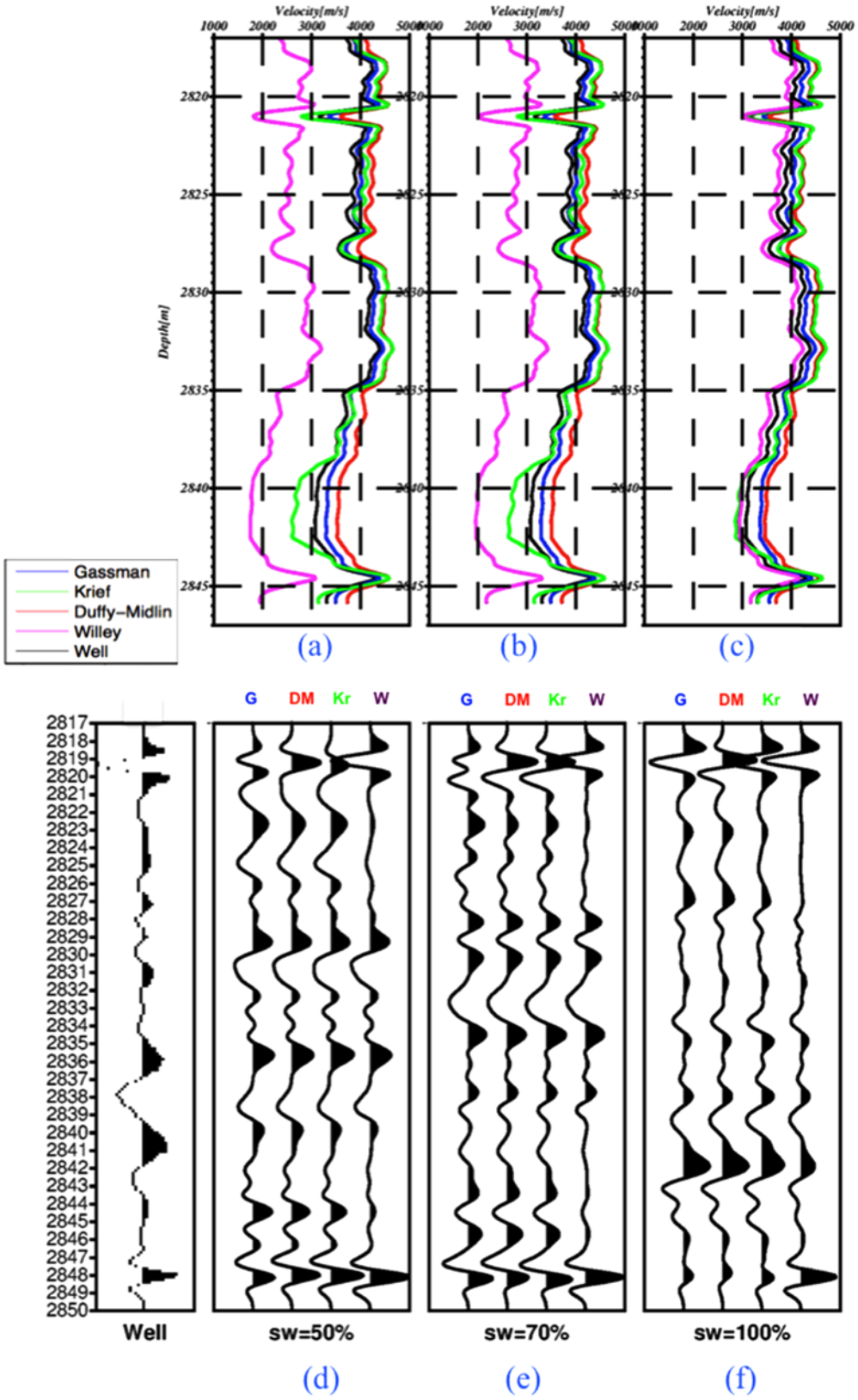

Fig. 8. Comparison of synthetic seismic traces at 50%, 70% and 100% water saturation scenarios. The well velocity is also drawn for comparison. Velocity obtained from different rock physics models at different water saturations is in top row (a, b, c). Synthetic seismic traces of well and corresponding synthetic traces in bottom row (d, e, f). Same colour conventions are used for velocity graphs and synthetic traces labelling.

http://dx.doi.org/10.1007/s12303-016-0041-x

For less porous zone Krief and Duffy-Mindlin's model not only exhibit the same trend in velocity with increasing water saturation but also their velocity values are very close to each other (Fig. 7a). For more porous zone Krief's model exhibit increase in velocity with increasing water saturation which is more pronounced at higher water saturations (Fig. 7b) while the Duffy-Mindlin's model shows slight decrease in velocity with increasing water saturation (Fig. 7b).

The response of different rock physics models at specific water saturations (50%, 70% and 100%) are compared in detail in terms of velocity and seismic synthetic traces (Fig. 8).

For 50% water saturation scenario (Fig. 8a), Duffy-Mindlin model predicts highest velocity while Wyllie's model predicts the lowest velocity. Krief's model also shows an increase in velocity except in the most porous zone (2838–2844 m). The synthetic traces for 50% water saturation level are shown in Figure 8d where Wiley's model synthetic trace is out of phase at the starting depth interval. Due to smaller velocity difference the synthetic traces of all models except Wyllie's model seems identical.

For the 70% water saturation scenario (Figs. 8b and e), the situation is similar to that for the 50% water saturation however with a slight increase in velocities. The Gassmann and Wyllie's model synthetic seismic traces are different from Duffy-Mindlin and Krief's model. Also note the change of reflection events and their amplitudes at synthetic seismic traces compared to 50% water saturation.

At 100% water saturation (Figs. 8c and f), the velocity of Wyllie's model is considerably higher as compared to other saturation levels but still lower than the well velocity (Fig. 8c). Duffy-Mindlin model shows the highest velocity value at 100% water saturation (Fig. 8c) while Krief's model shows a proportional decrease in velocity in most porous zone. The synthetic seismogram from Wyllie's model is in phase to the rest of the synthetic traces at 100% water saturation while the synthetic seismogram of Duffy-Mindlin's model is out of phase at depth of 2819m. For all levels of water saturation, the velocity obtained from Gassmann's model closely follows the velocity trend of Duffy-Mindlin's model.

Changes in impedances due to fluid substitution are manifested by seismic amplitude in the context of 4D seismic. However the position of reflections and strength of reflection amplitude will depend on the contrasts of adjacent acoustic impedances in the vertical succession.

For different water saturations the synthetic seismograms (Figs. 8d–f) show changes in position of reflections and their amplitudes strengths. For the depth interval of 2827–2830 m the change in reflection positions and their amplitude is evident for different water saturations compared to well synthetic seismogram. Similar changes are also evident at other depth intervals. At same water saturation the synthetic seismograms for different models show smaller difference in reflection amplitude, due to smaller velocity difference, but the changes in position of reflections and their amplitudes are pronounced significantly at different water saturations (Figs. 8d–f).

The limitation of this study mainly lies in the estimation of effective dry bulk modulus Kd. A common approach for the estimation of Kd while working with wireline log data is application of inverse Gassmann equation (Zhu and McMechan, 1990; Smith et al., 2003). We have followed the same approach for estimation of Kd, since no laboratory data was available. There are four critical parameters on which estimation of Kd depends namely porosity (obtained from well logs in this study), water saturation (obtained from well logs in this study), fluid properties, using Batzle and Wang (1992) relations at in situ conditions) and lithology (obtained by Voigt-Ruess-Hill (VRH) averaging using standard values of bulk and shear modulus for sand and shale).

The uncertainties in the above mentioned critical parameters lead to errors in calculated value of Kd. This is probably one of the major reasons that our modelled velocity response does not match with original well velocity curve. This can be avoided by proper calibration of modelled velocity response with the original well velocity curve, which requires detailed laboratory data (not available in this study). However, the modelled velocity response in this study nevertheless predicts the correct trend. This fits very well with the main focus of the paper about investigation of change in seismic amplitude with change of saturation within the context of 4D seismic study.

4. CONCLUSIONS

Rock physics models are used simultaneously to monitor quantify and predict the changes in reservoir properties. The accomplishment of these tasks depends on the careful computation of core parameters and physical well parameters are justified and linked to a particular scenario. Different rock physics model comparisons leads to better understanding of reservoir properties in a number of ways. The simplicity and efficiency of a rock physics model outweighs the rigorous and complex models at the stack of end results. This stems from the idea that comparing different rock physics models generates quantitative insights. In this study we have investigated and compared the predictions of four widely used rock physics models for clastic reservoir within the context of 4D seismic analyses.

The results of four rock physics models on the same real well log data are different due to the building physical parameters of the models. For all the models under study, except Wyllie's

model, the velocity calculated from well logs is lower than the velocity calculated from the respective models at same level of water saturation. The velocity varies in a narrow range for respective water saturations and this holds for all the rock physics models. The Krief's model is of particular importance, as it acts differently with in porous and most porous zone. There is sudden systematic decrease in velocities in the most porous zone. The possible explanation of this phenomenon may be attributed to the Biot's compressibility factor. This model may be used effectively to map the changes in most porous zone of a reservoir from less porous zone and further 4D interpretation. The response of Duffy-Mindlin's model closely resembles to the Gassmann's model but has overall higher velocities for respective saturations. Although this model is based on different physical parameters by considering the elastic moduli and overburden pressure nonetheless its striking similarity to Gassmann's model may lies in the utility of saturated bulk modulus that is determined from Gassmann's equation. The similar results are obtained even after using the bulk saturated modulus calculated from Krief's model.

It is hard to say which model would be preferred and under which circumstances. Perhaps more case studies will help to reach a definitive decision or at least show in detail the preference of one model over the others model albeit to the well conditions. Except the Krief's model, none of the model discriminates clearly the porous zones. From this study, the threshold porosity value is around 20% above that the velocities calculated from Krief's model decrease enormously.

ACKNOWLEDGMENTS

We are thankful to DGPC for providing the well data for this research. We are also thankful to the anomalous reviewers for reviewing the manuscript and their constructive suggestions to improve the quality of the research paper.

REFERENCES

Adam, L., Batzle, M., and Brevik, I., 2006, Gassmann's fluid substitution and shear modulus variability in carbonates at laboratory seismic and ultrasonic frequencies. Geophysics, 71, F173–F183.

Akhter, G., Ahmed, Z., Ishaq, A., and Ali, A., 2014, Integrated interpretation with Gassmann fluid substitution for optimum field development of Sanghar area, Pakistan: a case study. Arabian Journal of Geosciences, 8, 7467–7497.

Artola, F.A. and Alvarado, V., 2006, Sensitivity analysis of Gassmann's fluid substitution equations: Some implications in feasibility studies of time-lapse seismic reservoir monitoring. Journal of applied geophysics, 59, 47–62.

Avseth, P., Mukerji, T., and Mavko, G., 2005, Quantitative seismic interpretation: Applying rock physics tools to reduce interpretation risk (2nd edition). Cambridge University Press, Cambridge, 376 p.

Banks, C.J. and Warburton, J., 1986, Passive-roof duplex geometry in the frontal structures of the Kirthar and Sulaiman mountain belts, Pakistan. Journal of Structural Geology, 8, 229–237.

Batzle, M. and Wang, Z., 1992, Seismic properties of pore fluids. Geophysics, 57, 1396–1408.

Benson, S.M. and Cole, D.R., 2008, CO_2 sequestration in deep sedimentary formations. Elements, 4, 325–331.

Biondi, B., Mavko, G., Mukerji, T., Rickett, J., Lumley, D., Deutsch, C., Gundeso, R., and Thiele, M., 1998, Reservoir monitoring: a multidisciplinary feasibility study. The Leading Edge, 17, 1404–1414.

Biot, M.A., 1941, General theory of three-dimensional consolidation. Journal of Applied Physics, 12, 155–164.

Biot, M.A., 1956, Theory of propagation of elastic waves in a fluid-saturated porous solid. I. Low-frequency range. The Journal of the Acoustical Society of America, 28, 168–178.

Blonk, B., Calvert, R.W., Koster, J.K., and van der Zee, G., 1998, Assessing the feasibility of a 4D seismic reservoir monitoring project. Proceedings of European Petroleum Conference of the Society of Petroleum Engineers, Hague, Oct. 20–22, p. 307–314.

Castagna, J.P., Batzle, M.L., and Eastwood, R.L., 1985, Relationships between compressional-wave and shear-wave velocities in clastic silicate rocks. Geophysics, 50, 571–581.

Duffy, J. and Mindlin, R., 1957, Stress-strain relations and vibrations of a granular medium. Journal of Applied Mechanics, 24, 585–593.

Gassmann, F., 1951, Uber die Elastizität poröser median. Vierteljahrsschrift der Naturforschenden Gesellschaft in Zürich, 96, 1–23.

Geertsma, J. and Smit, D.C., 1961, Some aspects of elastic wave propagation in fluid-saturated porous solids. Geophysics, 26, 169–181.

Goldberg, I. and Gurevich, B., 1998, A semi-empirical velocity-porosity-clay model for petrophysical interpretation of P- and S-velocities. Geophysical Prospecting, 46, 271–285.

Guéguen, Y., 1994, Introduction to the Physics of Rocks. Princeton University Press, Princeton, 294 p.

Han, D. and Batzle, M.L., 2004, Gassmann's equation and fluid-saturation effects on seismic velocities. Geophysics 69, 398–405.

Han, D.H., Nur, A., and Morgan, D., 1986, Effects of porosity and clay content on wave velocities in sandstones. Geophysics, 51, 2093–2107.

Hashin, Z. and Shtrikman, S., 1963, A variational approach to the theory of the elastic behaviour of multiphase materials. Journal of the Mechanics and Physics of Solids, 11, 127–140.

Hill, R., 1952, The elastic behaviour of a crystalline aggregate. Proceedings of the Physical Society. Section A, 65, 349–354.

Johnston, D.H., 2013, Practical applications of time-lapse seismic data. Distinguished Instructor Series No. 16, Society of Exploration Geophysicists, 270 p.

Jones, T. and Nur, A., 1983, Velocity and attenuation in sandstone at elevated temperatures and pressure. Geophysical Research Letters, 10, 140–143.

Kadri, I.B., 1995, Petroleum Geology of Pakistan. Pakistan Petroleum Limited, Karachi, 275 p.

Kazemeini, S.H., Juhlin, C., and Fomel, S., 2010, Monitoring CO_2 response on surface seismic data; a rock physics and seismic mod-

 http://dx.doi.org/10.1007/s12303-016-0041-x

elling feasibility study at the CO_2 sequestration site, Ketzin, Germany. Journal of Applied Geophysics, 71, 109–124.

Krief, M.J., Garat, J., Stellingwerff, J., and Ventre, J., 1990, A petrophysical interpretation using the velocities of P and S waves (full waveform sonic). The Log Analyst, 58, 355–369.

Kumar, D., 2006, A tutorial on Gassmann fluid substitution: formulation, algorithm and Matlab code. Geohorizons, 4, 4–12.

Landrø, M., 2006, Future challenges and unexplored methods for 4D seismic analysis. Canadian Society of Exploration Geophysicists (CSEG), 31, 128–135.

Li, S., 2009, Characteristics of fluid substitution in porous rocks. Petroleum Science, 6, 139–145.

Lumley, D., 2001, Time-lapse seismic reservoir monitoring. Geophysics, 66, 50–53.

Mavko, G., Chan, C., and Mukerji, T., 1995. Fluid substitution: Estimating changes in Vp without knowing Vs. Geophysics, 60, 1750–1755.

Mavko, G., Mukerji, T., and Dvorkin, J., 2009, The Rock Physics Handbook: Tools for Seismic Analysis of Porous Media. Cambridge University Press, Cambridge, 511 p.

Mezghani, M., Fornel, A., Langlais, V., and Lucet, N., 2004, History matching and quantitative use of 4D seismic data for an improved reservoir characterization. Annual Technical Conference and Exhibition of Society of Petroleum Engineers, Houston, Sep. 26–29. http://dx.doi.org/10.2118/90420-MS

Misaghi, A., Negahban, S., Landr, M., and Javaherian, A., 2010, A comparison of rock physics models for fluid substitution in carbonate rocks. Exploration Geophysics, 41, 146–154.

Murphy, W.F., 1982, Effects of microstructure and pore fluid on the acoustic properties of granular sedimentary materials. Ph.D. thesis, Stanford University, Stanford, 255 p.

Nguyen, P.K. and Nam, M.J., 2011, A review on methods for constructing rock physics model of saturated reservoir rock for time-lapse seismic. Geosystem Engineering 14, 95–107.

de Paula, O.B., Pervukhina, M., and Gurevich, B., 2010, Testing Gassmann fluid substitution in carbonates: sonic log versus ultrasonic core measurements. 80th Annual International Meeting of Society of Exploration and Geophysics (Expanded Abstract), Denver, Oct. 17–22, p. 2670–2674.

Saleh, A. and Castagna, J., 2004, Revisiting the Wyllie time average equation in the case of near spherical pores. Geophysics, 69, 45–55.

Sengupta, M., Mavko, G., and Mukerji, T., 2003, Quantifying sub resolution saturation scales from time-lapse seismic data: A reservoir monitoring case study. Geophysics, 68, 803–814.

Simm, R., 2007, Practical Gassmann fluid substitution in sand/shale sequences. First Break, 25, 61–68.

Smith, T.M., Sondergeld, C.H, and Rai, C.S., 2003, Gassmann fluid substitutions: A tutorial. Geophysics, 51, 430–440.

Tsuneyama, F. and Mavko, G., 2007, Quantitative detection of fluid distribution using time-lapse seismic. Geophysical Prospecting, 55, 169–184.

Varela, O.J., Torres-Verdn, C., Sen, M.K., and Roy, I.G., 2006, Using time-lapse seismic amplitude data to detect variations of pore pressure and fluid saturation due to oil displacement by water: a numerical study based on one-dimensional prestack inversion. Journal of Geophysics and Engineering, 3, 177–193.

Wang, Z., 2001, Fundamentals of seismic rock physics. Geophysics, 66, 398–412.

Watts, G., Jizba, D., Gawith, D., and Gutteridge, P., 1996, Reservoir monitoring of the Magnus field through 4D time-lapse seismic analysis. Petroleum Geoscience, 4, 361–372.

Wood, A.W., 1955, A Textbook of Sound. McMillan Co., New York, 610 p.

Wyllie, M., Gregory, A., and Gardner, L., 1956, Elastic wave velocities in heterogeneous and porous media. Geophysics, 21, 41–70.

Wyllie, M., Gregory, A., and Gardner, G., 1958, An experimental investigation of factors affecting elastic wave velocities in porous media. Geophysics, 23, 459–493.

Zaigham, N.A. and K.A. Mallick., 2000, Prospect of hydrocarbon associated with fossil-rift structures of the southern Indus basin, Pakistan. American Association of Petroleum Geologists Bulletin, 84, 1833–1848.

Zhu, X. and McMechan, G.A., 1990, Direct estimation of the bulk modulus of the frame in a fluid saturated elastic medium by Biot's theory. 60th Annual International Meeting of Society of Exploration and Geophysics (Expanded Abstract), San Francisco, Sep. 23–27, p. 787–790.